Supporting Information

Jutras et al. 10.1073/pnas.1302351110

SI Methods

Procedures were carried out in accordance with National Institutes of Health guidelines and were approved by the Emory University Institutional Animal Care and Use Committee. Neuronal recordings were carried out in two adult male rhesus monkeys (*Macaca mulatta*) that were obtained from the breeding colony at the Yerkes National Primate Research Center. Their mean weight at the start of the experiment was 6.8 ± 1.1 kg, and their mean age was 4 y and 5 mo. Before implantation of recording hardware, monkeys were scanned with MRI to localize the hippocampus and to guide placement of the recording chamber. Using this information, a cilux plastic chamber (Crist Instrument Co.) for recording neural activity and a titanium post for holding the head were surgically implanted. We performed postsurgical MRI to fine-tune electrode placement and to determine recording locations.

Behavioral Testing Procedures. During testing, each monkey sat in a dimly illuminated room, 60 cm from a 19-inch cathode ray tube monitor running at 120 Hz at a noninterlaced refresh rate. Eye movements were recorded using a noninvasive IR eye-tracking system (ISCAN). Stimuli were presented using experimental control software (CORTEX, www.cortex.salk.edu). At the beginning of each recording session, the monkey performed a calibration task, which involved holding a touch-sensitive bar while fixating a small (0.3°) gray square presented on a dark background at various locations on the monitor. The monkey had to maintain fixation within a 3° window until the fixation point changed to an equiluminant yellow at a randomly chosen time between 500 ms and 1,100 ms after fixation onset. The monkey was required to release the touch-sensitive bar within 500 ms of the color change for delivery of a drop of applesauce. During this task, the gain and offset of the oculomotor signals were adjusted so that the computed eye position matched targets that were a known distance from the central fixation point.

Visual Preferential Looking Task. Following the calibration task, the monkey was tested on the visual preferential looking task (VPLT). The monkey initiated each trial by fixating a white cross (1°) at the center of the computer screen. After maintaining fixation on this target for 1 s, the target disappeared and a picture stimulus was presented (11°). The stimulus disappeared when the monkey's direction of gaze moved off the stimulus or after a maximum looking time of 5 s. Each stimulus was presented twice during a given session, with up to 8 intervening stimuli between successive presentations. The VPLT was given in 51 daily blocks of 6, 8, or 10 trials each, chosen pseudorandomly, for a total of 400 trials each day. The median delay between successive presentations was 8.1 s. Stimuli were obtained from Flickr (www.flickr.com). A total of 9,000 stimuli were used in this study.

Because the monkey controlled the duration of stimulus presentation, the duration of gaze on each stimulus provides a measure of the monkey's preference for the stimulus. We compared the amount of time the monkey spent looking at each stimulus during its first ("novel") and second ("repeat") presentations. Adult monkeys show a strong preference for novelty; therefore, a significant reduction in looking time between the two presentations of a stimulus indicated that the monkey had formed a memory of the stimulus and spent less time looking at the now familiar stimulus during its second presentation. To control for varying interest in individual stimuli, recognition memory performance was calculated as the difference in looking time between presentations as a percentage of the amount of time the monkey spent looking at the first presentation of each stimulus: (Novel − Repeat) ÷ Novel.

Reward was not delivered during blocks of the VPLT; however, five trials of the calibration task were presented between each block to give the monkey a chance to earn some reward and to verify calibration. The number of trials in each VPLT block was varied to prevent the monkey from knowing when to expect the rewarded calibration trials.

Electrophysiological Recording Methods. The recording apparatus consisted of a multichannel microdrive (FHC, Inc.) holding a manifold consisting of a 23-gauge guide tube containing four independently moveable tungsten microelectrodes (FHC, Inc.), with each electrode inside an individual polyamide tube. Electrode impedance was in the range of 1–2 MΩ, and electrode tips were separated horizontally by 190 μm. For each recording, the guide tube was slowly lowered through the intact dura mater and advanced to ∼3.5 mm dorsal to the hippocampus with the use of coordinates derived from the MRI scans. The electrodes were then slowly advanced out of the guide tube to the hippocampus. No attempt was made to select neurons based on firing pattern. Instead, we collected data from the first neurons we encountered in the hippocampus. At the end of each recording session, the microelectrodes and guide tube were retracted. All recordings took place in the anterior part of the left hippocampus (1). Recording sites were located in the CA3 field, dentate gyrus, and subiculum.

Data amplification, filtering, and acquisition were performed with a multichannel acquisition processor system from Plexon, Inc. The neural signal was split to extract the spike and the local field potential (LFP) components separately. For spike recordings, the signals were filtered from 250 Hz to 8 kHz, further amplified, and digitized at 40 kHz. A threshold was set interactively to separate spikes from noise, and spike waveforms were stored in a time window from 150 μs before to 650 μs after threshold crossing. Each recording typically yielded two to six units; single units were sorted offline using Offline Sorter (Plexon, Inc.). For LFP recordings, the signals were filtered with a passband of 0.7–170 Hz, further amplified, and digitized at 1 kHz; any additional filtering was performed in MATLAB (The Mathworks, Inc.). Only LFPs obtained from electrodes on which single-unit activity was also recorded were analyzed to ensure that all LFP data were taken from cell layers of the hippocampus. Eye movement data were digitized and stored with a resolution of 240 Hz.

Data Analysis. All analyses were performed using custom programming in MATLAB and using FieldTrip (fieldtrip.fcdonders.nl), an open-source toolbox for the analysis of neurophysiological data.

Saccade Detection. Eye movement data were analyzed to isolate fixation periods occurring between saccades. Saccades were detected by first applying a low-pass filter with a high-cut frequency limit of 40 Hz to the horizontal and vertical eye position data to remove high-frequency noise, differentiating and combining these signals to obtain the eye velocity, and setting a threshold of 40°/s to define saccades. The start and end of each saccade were considered to occur when the first-order derivative of the eye velocity (i.e., acceleration) reached zero before the upward crossing and after the downward crossing of this threshold, respectively.

Powerline Artifact Removal. We estimated the amplitude of the power-line fluctuations with a discrete Fourier transformation (DFT) of long data segments that contained the data epochs of interest. We then computed the DFT at 60 and 120 Hz. Because the power-line artifact is of a perfectly constant frequency and amplitude, and because the long data segments contained integer cycles of the artifact frequencies, essentially all the artifact energy is contained in those DFTs. We constructed sine waves with the amplitudes and phases as estimated by the respective DFTs and subtracted those sine waves from the original long data segments. The epoch of interest was then cut out of the cleaned epoch. Power spectra of the cleaned epochs demonstrated that all artifact energy was eliminated, leaving a notch with a bin width of 0.1 Hz in the monkey recordings.

Single-Unit Saccade Modulation. We recorded from 131 hippocampal single units in two monkeys. For each neuron, the firing activity aligned to saccades was examined by calculating perisaccade time histograms for the 1-s period centered at the onset of each saccade. We used a template matching procedure to test the modulation of the firing response following saccades for each neuron (2). Spike counts from the 300-ms period following each saccade were partitioned into 15 bins of 20 ms each, and the average baseline firing rate from the 300-ms period before saccade onset was subtracted from each bin. In this way, a 15-element vector was calculated for each saccade. The consistency of response patterns across saccades was determined by calculating the dot product of the vector for each saccade and the 15-element vector created by averaging all other response vectors (i.e., the average of vectors for all saccades, excluding the saccade under consideration). The products from all bins were then added together to produce a dot product measure for each saccade:

$$M_i = \sum_{j=1}^{15}\left(y_{ij} \times \sum_{k=1,\neq i}^{n} y_{kj}\right),$$

where n is the number of saccades in the dataset, M_i is the dot product measure for saccade i, y_{ij} is the amplitude of the response for saccade i and bin j (measured with respect to the presaccade baseline), and y_{kj} is the same as y_{ij} with index k substituted for index i. A test of proportions (3) was used to determine if the percentage of saccades for which the dot product measure, M_i, had positive values was significantly greater than 50%, according to the formula

$$z = \frac{\hat{p} - p}{\sqrt{\frac{p(1-p)}{n}}},$$

where $\hat{p}$ is the observed proportion of saccades for which M_i is positive, p is the hypothesized proportion, and n is the sample size. Fifty percent is the value expected by chance if there is no consistent response across saccades; thus, a value significantly greater than 50% indicates predictive power from calculating the average response to all other saccades. A one-tailed test with $\alpha = 0.01$ was used, corresponding to a critical z-value of 2.33.

LFP Spectral Analysis and Bout Detection. We calculated power spectra from LFP data after first limiting data segments to those recorded during blocks of VPLT performance, including intertrial intervals, prestimulus fixation periods, and stimulus presentation/exploration periods. Initial spectral analysis was performed using the multitaper method (4, 5) on nonoverlapping LFP segments of 5 s each, multiplying each with three orthogonal taper functions before Fourier transformation. This provided spectral smoothing of ±0.4 Hz. Local maxima were detected using the *localmax* function in MATLAB, designating a minimum peak distance of 1.6 Hz.

Bouts of theta activity in LFP data were quantified using an oscillatory episode detection algorithm that estimates the background power spectrum of the LFP to determine power and duration criteria (6–9). LFP segments were taken from blocks of VPLT performance, with each segment consisting of a block in its entirety (median block duration across all recordings was 32.5 s). After isolating LFP segments recorded during blocks of VPLT performance, we wavelet-transformed the raw LFP traces using Morlet wavelets with a window of seven cycles (10). As a result, for each frequency f, $7/(2f)$ s at the beginning and the end of each block were excluded from the calculation of wavelet power. Frequencies were sampled at 35 logarithmically spaced steps between 2 and 38 Hz. The background power spectrum for each LFP was determined by fitting a linear regression to this wavelet power spectrum in log–log coordinates. At each frequency, a power threshold, P_T, was set to the 95th percentile of the χ^2 (2) distribution of wavelet power values at that frequency and a duration threshold, D_T, was set to three cycles. For each frequency, all time intervals during which LFP power exceeded P_T for a time period exceeding D_T cycles were designated oscillatory episodes. Theta bouts were defined as any contiguous time points of oscillatory episodes within the 3- to 12-Hz frequency band (3.08–12.34 after $\log_2$ spacing). Finally, we defined P_{episode} as the proportion of time periods across all blocks of VPLT performance that exceeded both thresholds.

Data used to plot example theta bouts in Fig. 1 underwent a prewhitening step before wavelet multiplication/Fourier transformation for presentation. The example time-frequency spectrograms shown in Fig. 1*F*, and the corresponding autocorrelograms in Fig. 1*G*, were calculated from the following (from left to right): an LFP segment starting during the intertrial interval and persisting through the prestimulus fixation period; a segment starting during the prestimulus fixation period and ending shortly after stimulus onset; and two LFP segments occurring entirely within the stimulus presentation (free-viewing) period.

Theta Phase Resetting with Saccade Onset. To examine phase resetting of theta oscillations during the prestimulus fixation period, we selected trials in which the monkey did not make any saccades in the 600-ms period before the appearance of the center cross or in the 1,000-ms period between the saccade to the center cross and the onset of the stimulus. Because the monkey was only required to fixate within a 4° window around the center cross, it was possible in some excluded trials for a small saccade to occur during the prestimulus fixation period without aborting the trial. An average of 20.3 ± 2.2 trials per session met these criteria, representing, on average, 10.4% of trials in each session. Power values were calculated for the presaccade period (the 600-ms period preceding saccade onset) and the postsaccade period (the 600-ms period following a 400-ms postsaccade "buffer" period) using separate methods to obtain individual trial power measures and trial-averaged power measures. For individual trial power measures, we multiplied the raw LFP traces for each 600-ms period with one orthogonal taper function before Fourier transformation, providing spectral smoothing of ±1.67 Hz. We then calculated the average power in the 6.7- to 11.6-Hz frequency band, across trials, to obtain a theta power value for each LFP for presaccade and postsaccade periods. For trial-averaged power measures, the same method was used, with the exception that before taper multiplication and Fourier transformation, we calculated the average LFP signal (i.e., evoked signal) across trials. This resulted in a single trial-averaged segment for the 600-ms presaccade period for each LFP and another single trial-averaged segment for the 600-ms postsaccade period for each LFP. We then applied taper multiplication and Fourier transformation to each

LFP segment and calculated the average power in the 6.7- to 11.6-Hz frequency band, producing a theta power value for presaccade and postsaccade trial-averaged signals. A paired t test was used to determine whether theta power was significantly different for pre- and postsaccade periods, separately for individual trial theta power values and trial-averaged theta power values.

To calculate phase concentration for pre- and postsaccade LFPs, each LFP signal [encompassing the entire recording (i.e., before separating into pre- and postsaccade segments)] was first filtered with a band-pass filter of 6–12 Hz, using a zero–phase-shift fourth-order Butterworth filter. LFP segments were designated, which included 1,000 ms of presaccade LFP data and 1,300 ms of postsaccade LFP data. The local phase estimate at each time point in the LFP segment was calculated using the Hilbert transform, and phase distributions were calculated across all pre- and postsaccade fixation periods for each LFP channel. A 500-ms window was designated for the presaccade period, encompassing the period of −600 to −100 ms preceding saccade onset, allowing for a 100-ms buffer immediately preceding saccade onset to account for any distortion due to filtering. Similarly, a 500-ms window encompassing the period of 400–900 ms following saccade onset was designated for the postsaccade period. The degree of phase concentration across pre- and postsaccade fixation periods was evaluated by calculating the Rayleigh statistic (11) from the distribution of phases at each time point in each 500-ms window. Briefly, given n phases ϕ_i, the first trigonometric moment, $m = \left(\frac{1}{n}\right)\sum_{i=1}^{n} e^{j\phi_i}$, was defined. The preferred phase μ is given by the orientation of m, and the mean resultant value R is given by the modulus of m. The Rayleigh statistic is given by $Z = nR^2$. For each LFP, we calculated the average Rayleigh statistic value for the entire 500-ms window in each condition (pre- and postsaccade). A paired t test was used to determine the statistical significance of the difference in pre- and postsaccade Rayleigh statistic values.

Phase Distributions Following Saccade Onset During Visual Exploration. To examine the relationship between the LFP theta phase following saccade onset and recognition memory, the stimuli from each session were ranked in order of increasing recognition performance, quantified as the percentage of change in looking time between novel and repeat presentations for each stimulus. The 30 novel trials with the highest subsequent percentage of reduction were designated "high recognition" and the 30 novel trials with the lowest subsequent percentage of reduction were designated "low recognition." The first three postsaccade fixation periods in each trial were included in the analysis; thus, only those trials in which the monkey made at least three saccades during novel stimulus presentation, with each postsaccade fixation period lasting at least 200 ms, were used. This was done to control for the number of fixation periods in each condition and the amount of time included following each saccade. Finally, recording sessions in which fewer than 60 trials met these criteria were excluded from analysis to maintain an adequate separation between high recognition and low recognition conditions. Seventy-four LFP recordings met these inclusion criteria. Average looking times, latencies to the first saccade following stimulus onset, and intersaccade intervals for the first three 200-ms postsaccade fixation periods in each trial are presented in Table S1.

LFPs recorded during novel trials were filtered with a band-pass filter of 3–12 Hz, using a zero–phase-shift fourth-order Butterworth filter. LFP segments were designated, which included 500 ms of presaccade LFP data and 500 ms of postsaccade LFP data. The local phase estimate at each time point in this LFP segment was calculated using the Hilbert transform to extract the phase of the LFP at that time point. Phase distributions were calculated across all 90 postsaccade fixation periods in each condition for each LFP (the first 3 fixation periods taken from each of 30 trials in each condition). This ensured that the final distributions used for the statistical analysis contained an equal number of measurements. The degree of phase consistency across saccades was evaluated by calculating the Rayleigh statistic from the distribution of phases at each time point in the 400-ms window centered on saccade onset, for all the fixation periods in each condition, using methods described above. The probability that the null hypothesis of sample uniformity holds (i.e., the threshold for determining whether the phase distribution follows a random vs. nonuniform distribution) was calculated as $P = e^{-Z}$ (an adequate approximation for $n > 50$) (11, 12). For each LFP, we averaged the Rayleigh statistic values obtained in each condition for all time points falling between 40 and 200 ms after saccade onset. A paired t test was used to compare Rayleigh values between conditions across LFPs.

To evaluate the degree to which changes in postsaccade theta phase represent a reset in the phase of ongoing oscillatory activity rather than an additive, evoked response, we calculated power values for a 250-ms presaccade period and a 250-ms postsaccade period after first selecting saccades occurring during stimulus viewing that were not preceded by another saccade within a 400-ms window or followed by another saccade within a 250-ms window. This 400-ms presaccade window was chosen to prevent the inclusion of a potential evoked response during the preceding fixation period in the calculation of presaccade power, while still including a substantial number of trials for analysis. Within each recording session, an average of 40.2 ± 2.7 perisaccade periods met these criteria. Power values were calculated for the 250-ms periods preceding and following saccade onset, for individual trials (saccades) as well as, again, trial-averaged LFP segments. Each LFP segment was multiplied with one orthogonal taper function before Fourier transformation, providing spectral smoothing of ±4 Hz. After averaging power values across the range of theta-band frequencies (4–12 Hz), a paired t test was performed to compare theta power across LFPs for pre- and postsaccade periods, separately for individual trial power values and trial-averaged power values.

Theta Power Preceding Stimulus Onset and Relationship with Memory. To compare prestimulus theta power for subsequently well-recognized and subsequently poorly recognized stimuli, trials were ranked by increasing memory performance and the 30 trials with the largest/smallest difference in looking times between novel and repeat presentations were designated high recognition and low recognition (as above). Only those trials in which the monkey looked at the novel stimulus presentation for at least 750 ms were used. Each category represented a median of 22.2% of the total number of trials considered for each session. For each trial, the period of 800 ms immediately preceding stimulus onset was selected, buffered, and wavelet-transformed, using Morlet wavelets with a window of seven cycles. Time-frequency representations of spectral power were calculated from wavelet-transformed data segments, producing a mean time-resolved measure of spectral power for each LFP and each condition.

To test for statistical significance of differences in prestimulus theta power for high recognition and low recognition conditions, we performed a nonparametric multisample permutation test, with the median difference in power between conditions as our test statistic. The test involves a comparison of the observed difference against a reference distribution of differences under the null hypothesis of no significant modulation of power between conditions. The reference distribution was obtained by performing the following procedure 10,000 times. For each LFP, a random decision was made to which condition the data from either condition were assigned. We then calculated the test statistic at each time and frequency for these randomly assigned conditions and stored only the minimal and maximal differences across frequencies. From the resulting distribution of 10,000 minimal

and maximal differences, we determined the 2.fifth and the 97.fifth percentiles. The empirically observed, nonrandomized difference at a particular frequency was considered statistically significant ($P < 0.05$), when it was larger than the 97.fifth or smaller than the 2.fifth percentile of the reference distribution. This procedure corresponds to a two-sided test with a global false-positive rate of 5% and correction for the multiple comparisons across frequencies (13, 14). We used this nonparametric permutation approach, because (*i*) it is free of assumptions about the underlying distributions, (*ii*) it is not affected by partial dependence among the time-frequency tiles, and (*iii*) it allows for correction for multiple comparisons without additional assumptions.

To investigate the extent to which LFP data immediately following stimulus onset might have some influence on the enhancement in prestimulus theta-band power associated with better recognition memory, we designated 444-ms windows immediately preceding and immediately following stimulus onset for the same high recognition and low recognition trials. Each LFP segment was multiplied with a Hanning taper function before Fourier transformation. Because the band of memory-related prestimulus power enhancement was centered at 9 Hz, a paired *t* test was performed to compare power values at 9 Hz in each window across LFPs for the high recognition and low recognition conditions.

Theta Oscillations and Investigation of Phase Resetting During Calibration Task. To quantify the presence of theta-band activity during the calibration task, in which saccadic eye movements tend to be cued rather than exploratory, we applied the $P_{episode}$ analysis to data recorded during blocks of the calibration task. The methods for this analysis were identical to those used to quantify theta-band activity during blocks of the VPLT. The average theta $P_{episode}$ across LFPs, taken across all blocks of the calibration task, was 0.19 ± 0.01. Bouts of theta-band activity occurred with a median bout duration of 502 ms and a median interbout interval of 1,551 ms.

The extent to which the oscillatory phase was reset with the onset of cued saccades during the calibration task was investigated using analyses identical to those performed for saccades during the prestimulus period. Briefly, power values were calculated for the presaccade period (the 600-ms period preceding saccade onset) and the postsaccade period (the 600-ms period following a 400-ms postsaccade buffer period) using separate methods to obtain individual trial power measures and trial-averaged power measures (as described in *Methods*). Taper multiplication and Fourier transformation were used to calculate the average power in the 6.7- to 11.6-Hz frequency band for each LFP segment, producing a theta power value for presaccade and postsaccade trial-averaged signals. A paired *t* test was used to determine whether theta power was significantly different for pre- and postsaccade periods, separately for individual trial theta power values and trial-averaged theta power values.

We also calculated the Rayleigh statistic as follows: Each LFP signal (encompassing the entire recording) was filtered with a bandpass filter of 6–12 Hz. Saccades occurring following the appearance of the gray square in the calibration task were selected, and trials were limited to saccades that were followed by a fixation period lasting at least 1 s. LFP segments were designated, which included 1,000 ms of presaccade LFP data and 1,300 ms of postsaccade LFP data. The local phase estimate at each time point in the LFP segment was calculated using the Hilbert transform, phase distributions were calculated across all pre- and postsaccade fixation periods for each LFP channel, and the degree of phase concentration across pre- and postsaccade fixation periods was evaluated by calculating the Rayleigh statistic from the distribution of phases at each time point in the 500-ms windows designated for each period (−600 to −100 ms preceding saccade onset and 400–900 ms following saccade onset).

1. Jutras MJ, Fries P, Buffalo EA (2009) Gamma-band synchronization in the macaque hippocampus and memory formation. *J Neurosci* 29(40):12521–12531.
2. Sobotka S, Nowicka A, Ringo JL (1997) Activity linked to externally cued saccades in single units recorded from hippocampal, parahippocampal, and inferotemporal areas of macaques. *J Neurophysiol* 78(4):2156–2163.
3. Sokal RR, Rohlf FJ (1995) *Biometry* (Freeman, New York).
4. Jarvis MR, Mitra PP (2001) Sampling properties of the spectrum and coherency of sequences of action potentials. *Neural Comput* 13(4):717–749.
5. Mitra PP, Pesaran B (1999) Analysis of dynamic brain imaging data. *Biophys J* 76(2): 691–708.
6. Hughes AM, Whitten TA, Caplan JB, Dickson CT (2012) BOSC: A better oscillation detection method, extracts both sustained and transient rhythms from rat hippocampal recordings. *Hippocampus* 22(6):1417–1428.
7. Caplan JB, Madsen JR, Raghavachari S, Kahana MJ (2001) Distinct patterns of brain oscillations underlie two basic parameters of human maze learning. *J Neurophysiol* 86(1):368–380.
8. Ekstrom AD, et al. (2005) Human hippocampal theta activity during virtual navigation. *Hippocampus* 15(7):881–889.
9. van Vugt MK, Sederberg PB, Kahana MJ (2007) Comparison of spectral analysis methods for characterizing brain oscillations. *J Neurosci Methods* 162(1-2):49–63.
10. Grossman A, Morlet J (1985) Decomposition of functions into wavelets of constant shape, and related transforms. *Mathematics + Physics*, ed Streit L (World Scientific, Singapore).
11. Fisher NI (1993) *Statistical Analysis of Circular Data* (Cambridge Univ Press, Cambridge, UK).
12. Siapas AG, Lubenov EV, Wilson MA (2005) Prefrontal phase locking to hippocampal theta oscillations. *Neuron* 46(1):141–151.
13. Nichols TE, Holmes AP (2002) Nonparametric permutation tests for functional neuroimaging: A primer with examples. *Hum Brain Mapp* 15(1):1–25.
14. Maris E, Oostenveld R (2007) Nonparametric statistical testing of EEG- and MEG-data. *J Neurosci Methods* 164(1):177–190.

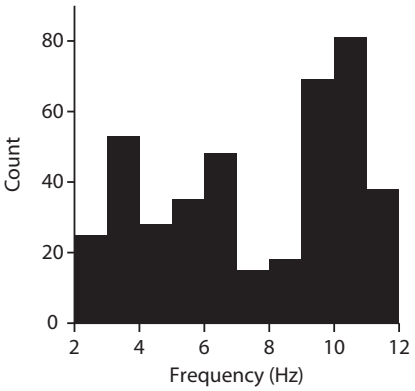

Fig. S1. Distribution of spectral peaks across hippocampal LFPs. The distribution of local maxima in the 2- to 12-Hz range in the power spectra of prewhitened LFP data was recorded on all channels during VPLT performance.

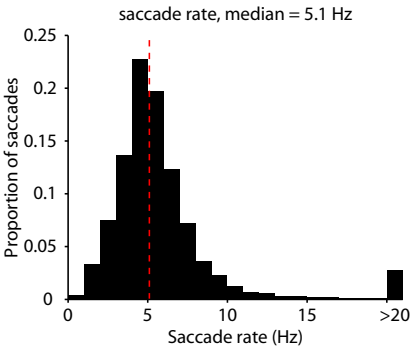

Fig. S2. Distribution of saccade rates across recordings. The distribution of saccade rates for all saccades was measured across 45 test sessions of the VPLT. The red dashed line indicates the median (5.1 Hz).

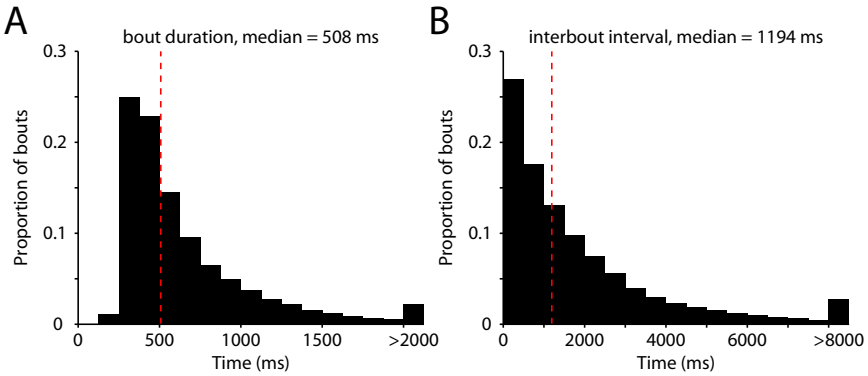

Fig. S3. Theta bout durations and interbout intervals. (*A*) Distribution of theta bout durations across 114 LFPs. The red dashed line indicates the median (508 ms). (*B*) Distribution of theta interbout intervals across 114 LFPs. The red dashed line indicates the median (1,194 ms).

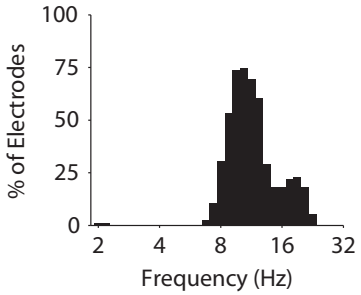

Fig. S4. LFPs display significant levels of oscillatory activity. The histogram shows the distribution of LFP channels with significant $P_{episode}$ values at each frequency tested (two-tailed t test, $P < 0.014$).

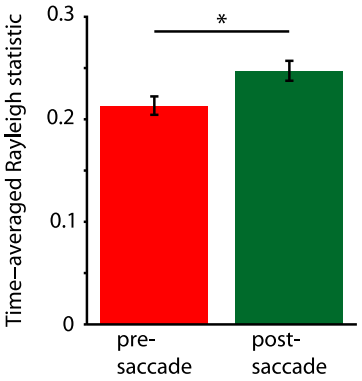

Fig. S5. Presaccade and postsaccade theta-band phase reliability during the prestimulus period. The average Rayleigh statistic values, representing phase reliability, for theta-filtered (6.7–11.6) LFP segments taken from the 500-ms presaccade (red) and postsaccade (green) periods during the prestimulus period are shown. Phase reliability was significantly higher for the postsaccade period than for the presaccade period (paired-sample t test, $*P < 0.01$).

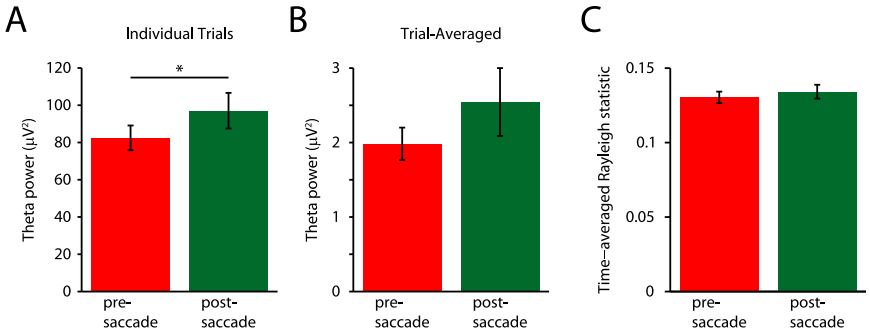

Fig. S6. Presaccade and postsaccade theta-band phase reliability during calibration task. Theta (6.7–11.6 Hz) power was calculated across all single trials (*A*) and for each trial-averaged signal (*B*) for presaccade (red) and postsaccade (green) periods. Theta power was significantly higher for the postsaccade period than for the presaccade period for the individual trial signals ($*P < 0.05$) but not for the trial-averaged signals ($P > 0.1$). (*C*) Average Rayleigh statistic values, representing phase reliability, for theta-filtered (6.7–11.6) LFP segments taken from the 500-ms presaccade and postsaccade periods.

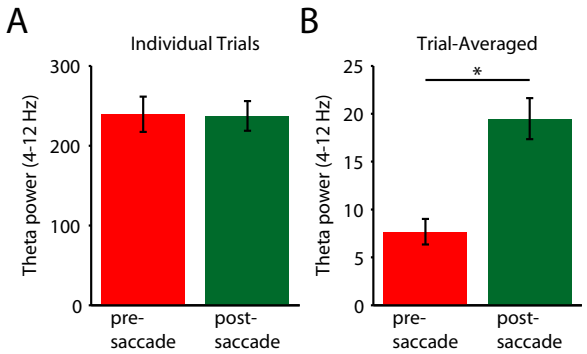

Fig. S7. Presaccade and postsaccade theta-band LFP power for individual saccades and for average saccade-locked LFPs. (*A*) Theta (4–12 Hz) power in the 250-ms window immediately preceding saccades (red) and immediately following saccades (green), calculated for individual LFP segments. (*B*) Theta power in 250-ms presaccade and postsaccade windows, calculated for LFP segments after averaging across all saccades in a session ($n = 87$ LFP channels). Theta power was significantly higher for the postsaccade period than for the presaccade period for the trial-averaged signals (*$P < 0.01$) but not for the individual trial signals ($P > 0.1$).

Table S1. Novel trial looking times, latency to first saccade following stimulus onset, and intersaccade intervals for the high recognition and low recognition conditions

Total no. of sessions ($n = 27$)	High recognition	Low recognition	*P* value
Novel trial looking time, ms	4,448.6 ± 43.0	2,818.4 ± 124.3	$P < 0.01$
Latency to first saccade after stimulus onset, ms	229.2 ± 2.4	226.6 ± 2.9	$P > 0.1$
Intersaccade interval, ms	241.3 ± 3.0	243.3 ± 2.8	$P > 0.1$

Measures are presented as the average ±SEM.